Correspondence/Rebuttal

# Selective PKC# inhibitor B106 elicits uveal melanoma growth inhibitory effects independent of activated PKC isoforms

Renier Heijkants, Amina Teunisse, Jelle de Vries, Huib Ovaa, and Aart Jochemsen

*ACS Chem. Biol.*, **Just Accepted Manuscript** • DOI: 10.1021/acschembio.8b00292 • Publication Date (Web): 07 Dec 2018

A

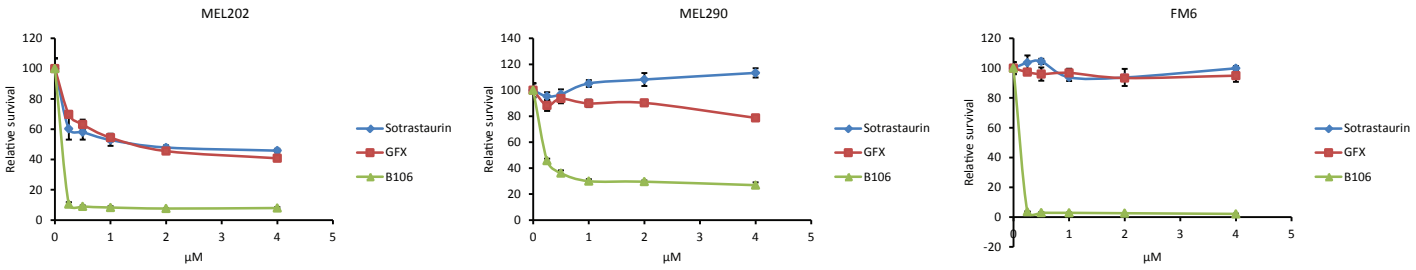
MEL202
MEL290
FM6
Relative survival
μM
Sotrastaurin
GFX
B106

B

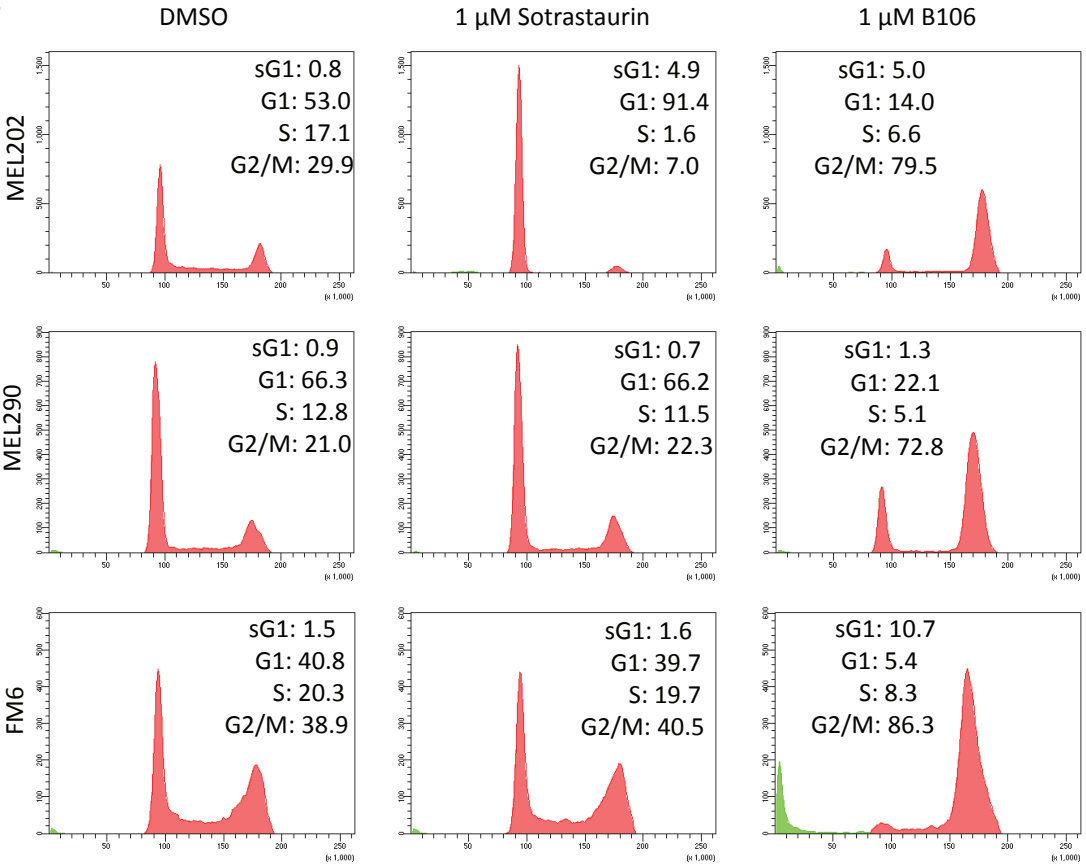
DMSO
1 μM Sotrastaurin
1 μM B106
MEL202
MEL290
FM6
sG1: 0.8
G1: 53.0
S: 17.1
G2/M: 29.9
sG1: 4.9
G1: 91.4
S: 1.6
G2/M: 7.0
sG1: 5.0
G1: 14.0
S: 6.6
G2/M: 79.5
sG1: 0.9
G1: 66.3
S: 12.8
G2/M: 21.0
sG1: 0.7
G1: 66.2
S: 11.5
G2/M: 22.3
sG1: 1.3
G1: 22.1
S: 5.1
G2/M: 72.8
sG1: 1.5
G1: 40.8
S: 20.3
G2/M: 38.9
sG1: 1.6
G1: 39.7
S: 19.7
G2/M: 40.5
sG1: 10.7
G1: 5.4
S: 8.3
G2/M: 86.3

C

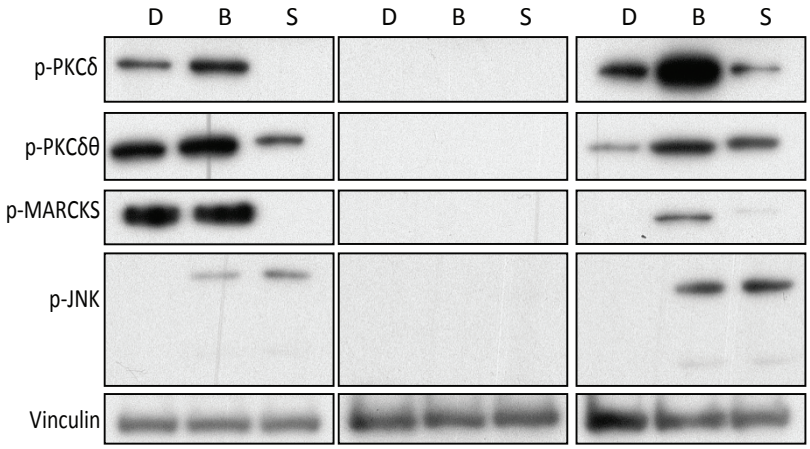
MEL202
MEL290
FM6
D
B
S
p-PKCδ
p-PKCδθ
p-MARCKS
p-JNK
Vinculin

D

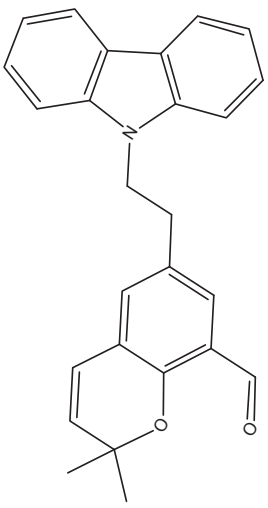

**Selective PKCδ inhibitor B106 elicits uveal melanoma growth inhibitory effects independent of activated PKC isoforms**

Renier Heijkants, Amina Teunisse, Jelle de Vries, Huib Ovaa and Aart Jochemsen.
Department of Cell and Chemical Biology.
Leiden University Medical Center.
Leiden, the Netherlands.

**Abstract**

In uveal melanoma (UM) cells the protein kinase C (pathway) is almost generally constitutively activated as a result of an activating mutation in either the GNAQ or the GNA11 G-protein. A pan-PKC inhibitor, Sotrastaurin (also named AEB071), is in clinical trials for treatment of UM patients with limited success and eliciting adverse effects. Interestingly, genetic interference with expression of just one PKC isoform, e.g. PKCδ, is sufficient to reduce UM cell proliferation. Therefore, we tested the effect of a recently described specific PKCδ inhibitor, B106, on growth and survival of UM cell lines. Surprisingly, we found that B106 efficiently induced apoptosis in several cell lines, but apparently independent of activated PKCδ.

Uveal melanoma (UM) is a lethal ocular malignancy, which is driven by oncogenic mutations in the α-subunits of G-proteins GNAQ or GNA11 [1, 2]. Activated GNAQ/11 are known to feed into various signaling pathways, including the activation of protein kinase C (PKC) isoforms [3-6]. Several studies have shown that activated PKCs are essential for UM cell proliferation [7, 8]. These results have spurred the use of pan-PKC inhibitors in the clinic to treat UM. Half of the patients show disease stabilization upon PKC inhibition, unfortunately all patients show adverse effects [9]. It has been demonstrated by genetic means that UM cells expression mutant GNAQ or GNA11 are, among other PKC isoforms, dependent on expression PKCδ [3, 7, 8, 10]. These results indicated that targeting of a single PKC isoform, e.g. PKCδ, by a specific small molecule compound rather than the pan-PKC inhibitor approach, could yield a similar therapeutic effect with potentially less adverse effects.

We noted that Takashima *et al.* (2014) reported the development of a selective PKCδ inhibitor named B106, which very efficiently induced apoptosis in cutaneous melanoma cell lines [11].

We reasoned that this particular inhibitor could be regarded as an interesting therapeutic potential for UM. To investigate this possibility, we tested the growth inhibitory effect of B106 on a panel of UM cell lines in comparison with two pan-PKC inhibitors, GF109203X (GFX) and the clinically used Sotrastaurin. Three of the tested cell lines contain either a GNAQ mutation (MEL202, OMM2.3) or a GNA11 mutation (MM66). The MEL285 and MEL290 cell lines do not contain a GNAQ or GNA11 mutation, although they are still regarded as uveal melanoma cell lines [12]. The three UM cell lines MEL202, OMM2.3 and MM66 were found to be growth inhibited by B106 treatment and even showed a greater sensitivity for B106 compared to both pan-PKC inhibitors (Fig 1A and Supplementary Fig 1A). In accordance with earlier observations, both MEL290 and MEL285 were resistant for pan-PKC inhibition correlating with the lack of PKC activity [13 8]. Surprisingly, these latter UM cell lines were still sensitive for B106 treatment, despite the absence of activated PKC isoforms and absence of phosphorylated MARCKS, a hallmark of the presence of active PKC protein(s).

As a comparison for B106 activity we made use of the NRAS mutated cell line FM6, which was also investigated in the study by Takashima *et al.* In accordance with the original study the FM6 cells were found to be very sensitive for B106, but were not growth inhibited by either Sotrastaurin or GFX, suggesting that activated PKC is not relevant for the proliferation of these cells (Figure 1A). To assess the effect of the compounds on cell cycle progression we performed flow cytometry analyses. Treatment with 1 μM Sotrastaurin for 24 hours induced G1 cell cycle arrest only in those cells containing a GNAQ or GNA11 activating mutation (MEL202, OMM2.3 and MM66; Fig 1B and Supplementary Fig 1B). Cell cycle profiles of FM6, MEL290 and MEL285 were hardly affected by Sotrastaurin. B106, on the other hand, induced a clear G2/Mitosis arrest in all cell lines, regardless of PKC activity (Fig 1B and Supplementary Fig 1B). These results suggested to us that the mode of action of B106 is independent of presence of activated PKC isoforms.

Takashima *et al.* showed that the activation of c-Jun N-terminal Kinases 1 and 2 (JNK), as assessed by increased phosphorylation is, at least partly, essential for the B106-induced apoptosis in NRAS mutated cutaneous melanoma cells [11]. To investigate the effect of B106 in comparison with Sotrastaurin on activation of JNK the cell lines were treated with 1 μM of B106 and 4 μM Sotrastaurin for 2 hours. Interestingly, both B106 and Sotrastaurin treatment increased phosphorylated JNK in all cell lines apart from MEL290 (Figure 1C and Supplementary Figure 1C). Whereas pan-PKC inhibition by Sotrastaurin reduced phosphorylation/activation of specific PKCδ and PKCδ/θ as well as the PKC phosphorylation substrate MARCKS, incubation with B106 did not reduce PKCδ- or MARCKS phosphorylation and in some cell lines phosphorylation of PKCδ was even found to be increased. These data indicate that B106 is inhibiting cell growth and survival, but that this effect can be observed independent on the presence of activated PKCδ in the cells and apparently also independent on the activation of JNK, as illustrated by the MEL290 cell line.

Takashima *et al.* show that B106 is a selective PKCδ inhibitor when compared to PKCα in a cell free system. However, it must be noted that in this *in vitro* kinase assay the IC50 for PKCδ is still 50 nM [11], which is relatively high compared to 2.1 nM for Sotrastaurin [14].

To obtain more insight into the mode-of-action of B106 as a kinase inhibitor, the compound was provided to a company to perform a kinome analysis. The effect of B106 was determined on the activity of 366 human kinases, at two concentrations, 0.1 μM and 1.0 μM. Surprisingly, hardly any kinase was inhibited by B106. MEK2 activity was reduced the most, to 56% at 1.0 μM while ROCK1 and PKCθ activities were reduced to 74% and 78%, respectively. PKCδ activity was not inhibited at all under these conditions (Supplementary tables 1 and 2). Because MEK2, which is upstream of ERK1/2, was identified as the most inhibited kinase in this assay, we determined the effect of B106 on ERK1/2 phosphorylation in comparison with Sotrastaurin. As reported before, [7, 8] Sotrastaurin decreased ERK1/2 phosphorylation but B106 actually slightly increased ERK1/2 phosphorylation (data not shown).

The result of the kinome profiling actually supports our data presented here and de-substantiates the claim that B106 is a PKCδ specific inhibitor.

We recognize the significance and potential high clinical impact of a selective PKCδ inhibitor. Unfortunately, it appears that B106 does not live up to the promise. Our results indicate that very likely a mode-of-action of B106 exists, distinct from simple kinase inhibition, yet to be elucidated.

How to explain the strong growth inhibitory and apoptosis-inducing activity of B106? Part of B106 is still similar to Rottlerin, the structure of which has been one of the starting points in the development of B106. Although Rottlerin was originally reported as a kinase inhibitor with some specificity for PKCδ, more recent studies highly question this specificity and one report even indicates that PKCs are completely insensitive to Rottlerin in a cell free assay [15, 16]. Soltoff indicates that among the various effects of Rottlerin it acts as a mitochondrial uncoupler, resulting in strongly reduced ATP levels in the cytoplasm, depolarisation of the mitochondrial membrane affecting ROS (Reactive Oxygen Species) levels and possibly inducing apoptosis [15, 17]. Although such effects have not been investigated for B106, it is not excluded that increased ROS levels contribute to the apoptosis inducing effects of B106, also because ROS do activate JNK via the ASK1-MKK4 pathway [18, 19]. Indeed, our preliminary data indicate that the increase in phosphorylated JNK is attenuated by incubation with N-acetyl-L-cysteine, a well-known ROS scavenger (data not shown).

We think it would be a possibility to employ similar techniques and approaches as Takashima *et al.* have employed but with Sotrastaurin as a starting scaffold for chemical modifications to make it more selective for PKCδ. Alternatively, recently a few publications describe the identification of isoform-specific PKC inhibitors, i.e. PKCι and PKCζ [20, 21]; possibly similar approaches could be used to develop PKCδ-specific inhibitor(s) to modify Sotrastaurin to make it more selective for PKCδ.

## Methods

### Cell culture

MEL202, MEL290, MEL285 and OMM2.3 were cultured in a mixture of RPMI and DMEM-F12 (1:1 ratio), supplemented with 10% foetal calf serum (FCS) and antibiotics [22]. MM66 cells were cultured in IMDM medium, supplemented with 15% FCS and antibiotics [6]. FM6 were cultured in DMEM, 10% FCS and antibiotics.

### Growth assays

Cells were seeded in triplicate, in 96-well format and incubated for 3 days with drugs as indicated. Cell survival was determined via the Cell Titre-Blue Cell Viability assay (Promega); fluorescence was measured in a micro plate reader (Victor, Perkin Elmer).

### Flow cytometry

Cells were incubated for 24 hours with 1 μM B106, 1 μM Sotrastaurin or vehicle (DMSO) and harvested by trypsinization. PBS was used to wash the cells twice before fixing them in ice cold 70% ethanol at -20 ºC for at least 16 hours. Subsequently, cells were washed in PBS containing 2% FCS and stained for 30 minutes at 37 ºC using PBS containing 2% FCS, 50 μg/ml RNAse and 50 μg/ml propidium iodide (PI). Analysis was performed on BD LSR II system (BD Biosciences).

### Western blot analysis

After a 2-hour incubation with 1 μM B106, 4 μM Sotrastaurin or vehicle (DMSO) cells were lysed in Giordano buffer (50 mM Tris-HCl pH 7.4, 250 mM NaCl, 0.1% Triton X-100 and 5 mM EDTA; supplemented with phosphatase- and protease inhibitors). Proteins were separated using SDS-PAGE

after which the proteins were blotted onto polyvinylidene fluoride transfer membranes (Millipore, Darmstadt, Germany). Blocking of the membranes was achieved using TBST (10 mM Tris-HCl pH8.0, 150 mM NaCl, 0.2% Tween 20) containing 10% milk. Membranes were incubated with the following primary antibodies: phospho-JNK (Thr183/Tyr185; Cat. #4668), phospho-MARCKS (Ser152/156; Cat. #2741), phospho-PKCδ (Thr505; Cat #9374), phospho-PKCδ/θ (Ser643/676; Cat. #9376) all from Cell Signaling Technology, and Vinculin (hVIN-1/V9131, Sigma-Aldrich) and appropriate HRP-conjugated secondary antibodies (Jackson Laboratories). Bands were visualized by exposure to X-ray film using chemoluminescence.

**Kinome analysis**

To determine the effect of B106 on activity of 366 human kinases, a stock of 10 mM of B106 dissolved in DMSO was shipped to Eurofins Pharma Discovery Services UK Limited. Effect of B106 was determined in the KinaseProfiler service.

**Preparation of B106**

Unless stated otherwise, all reagents were obtained from commercial suppliers and were used without further purification. All air or moisture sensitive reactions were performed under an argon or nitrogen atmosphere or under a positive flow of argon or nitrogen in heat gun- or vacuum oven-dried glassware. Tetrahydrofuran (THF) was obtained from an Inert (Amesbury, MA) dry solvent system (degassed solvents delivered through activated alumina columns, positive pressure of nitrogen). Acetonitrile (ACN) and Toluene were dried over activated 4Å molecular sieves. Deionized and degassed water ($H_2O$) was used for reactions. Column chromatography was performed with prepacked silica flash cartridges (GraceResolv, Grace Davison Discovery Science) on a Buchi Sepacore purification system (SepacoreControl 1.2 Chromatography Software, C-620 Control Unit, C-660 Fraction Collector, C-640 UV Photometer, C-605 Pump Modules, BÜCHI Labortechnik A). Nuclear magnetic resonance (NMR) spectra were recorded on a Bruker Ultrashield$^{TM}$ 300 (75.00 MHz for $^{13}C$) using the residual solvent as internal standard ($^{1}H$: δ 7.26 ppm, $^{13}C\{^{1}H\}$: δ 77.00 ppm for $CDCl_3$), Chemical shifts (δ) are given in ppm and coupling constants (*J*) are annotated in Hertz (Hz). Resonances are described as s (singlet), d (doublet), t (triplet), q (quartet), br (broad singlet) and m (multiplet) or combinations thereof. LC-MS measurements were performed on a system equipped with a Waters 2795 Separation Module (Alliance HT), Waters 2996 Photodiode Array Detector (190-750 nm) Phenomenex Kinetex C18 (2.1x50, 2.6 µm) and LCT$^{TM}$ ESI Mass Spectrometer. Electrospray Ionization (ESI) high-resolution mass spectrometry was carried out using a Waters Xevo G2 XS QTOF instrument in positive ion mode.

**Synthesis of 5-bromo-2-((2-methylbut-3-yn-2-yl)oxy)benzaldehyde:**

To a thoroughly dried 100 mL round bottomed flask containing 2-methylbut-3-yn-2-ol (5.54 mL, 57.2 mmol, 1.15 equiv.) dissolved in dry ACN (50 mL) at 0° C was added 1,8-Diazabicyclo[5.4.0]undec-7-ene (DBU, 11.1 mL, 74.6 mmol, 1.5 equiv.). To this mixture trifluoroacetic anhydride (8.08 mL, 57.2 mmol, 1.15 equiv.) was added dropwise over a 10 minute period. The reaction was stirred at 0° C for 45 minutes before being transferred *via cannula* to a 250 mL round bottomed flask containing 5-bromo-2-hydroxybenzaldehyde (10.0 g, 49.7 mmol, 1 equiv.), DBU (9.65 mL, 64.6 mmol, 1.3 equiv.)

and $CuCl_2.2H_2O$ (8.5 mg, 0.050 mmol, 0.001 equiv.) in ACN at -5° C. After 1,5 hours cooling was removed and the mixture was stirred at ambient temperature for 16 hours before being concentrated under reduced pressure at 40 °C. The resulting residue was taken up in ethyl acetate (EtOAc), washed once with $H_2O$, once with 1 M HCl and once with brine before being dried using $Na_2SO_4$, filtered and concentrated. This residue was adsorbed onto Celite and subjected to silica gel flash chromatography eluting with 0% to 50% EtOAc in heptane to yield 8.42 g (63%) of the desired product as a yellow solid.

$^1$H-NMR (300 MHz, $CDCl_3$) δ: 10.31 (s, 1H), 7.93 (d, *J* = 2.6 Hz, 1H), 7.59 (dd, *J* = 8.9, 2.65 Hz, 1H), 7.42 (d, *J* = 8.9 Hz, 1H), 2.63 (s, 1H), 1.71 (s, 6H) (Supplementary Figure 2A). $^{13}$C-NMR (75 MHz, $CDCl_3$) δ: 188.7, 157.1, 137.3, 130.7, 130.0, 122.6, 115.9, 84.4, 75.9, 74.3, 29.4. ESI+ MS: 267.0, 269.0 $[M+H]^+$ (data not shown).

**Synthesis of 6-bromo-2,2-dimethyl-2H-chromene-8-carbaldehyde:**

5-Bromo-2-((2-methylbut-3-yn-2-yl)oxy)benzaldehyde (1.0 g; 3.7 mmol; 1.0 equiv.) was taken up in ACN (15 mL)in a 20 mL microwave vial. Butylated hydroxytoluene (BHT, 16 mg; 0.075 mmol; 0.02 equiv.) was added and the mixture was heated at 180 °C for 20 minutes. Two more identical runs with additional fresh catalytic amounts of BHT were performed before the crude was adsorbed onto Celite and subjected to silica gel flash chromatography eluting with 0% to 25% EtOAc in heptane to yield 488 mg (49%) of the desired product.

$^1$H-NMR (300 MHz, $CDCl_3$) δ: 10.35 (s, 1H), 7.71 (d, *J* = 2.5 Hz, 1H), 7.26 (d, *J* = 2.5 Hz, 1H), 6.28 (d, *J* = 10.0 Hz, 1H), 5.75 (d, *J* = 10.0 Hz, 1H), 1.49 (s, 6H) (Supplementary Figure 2B). $^{13}$C-NMR (75 MHz, $CDCl_3$) δ: 187.8, 155.1, 134.1, 132.6, 129.2, 125.4, 124.3, 120.5, 113.1, 78.1, 28.1. ESI+ MS: 267.0, 269.0 $[M+H]^+$ (data not shown).

**Synthesis of 9-(2-(trifluoro-λ$^4$-boraneyl)ethyl)-9H-carbazole, potassium salt:**

In a thoroughly dried 100 mL round-bottomed flask 2,5-dimethyl-hexa-2,4-diene (4.11 mL; 27.4 mmol; 5.5 equiv.) was dissolved in THF (10 mL) and the mixture was cooled to 0 °C. A 1.0 M solution of $BH_3$.THF complex in THF (12.9 mL; 12.9 mmol; 2.5 equiv.) was added and the mixture was stirred at 0 °C for 3 hours. Then, a solution of 9-vinylcarbazole (1.0 g; 5.17 mmol; 1.0 equiv.) in THF (1 mL) was added. The reaction mixture was allowed to warm up to room temperature and stirred for an additional 3 hours before being cooled to 0 °C followed by addition of $H_2O$ (1.7 mL; 94 mmol; 18 equiv.). The mixture was stirred at ambient temperature for 1,5 hours before a 37% aq. formaldehyde solution (4.3 mL; 58 mmol; 11 equiv.) was added and the mixture was stirred at ambient temperature overnight. The reaction mixture was poured into brine (50 mL) and extracted with EtOAc (75 mL). The organic layer was separated, dried ($Na_2SO_4$), filtered and concentrated to dryness under reduced pressure at 40 °C to give 4.4 g of a colourless oil. The resulting oil was dissolved in acetone (17 mL) and $H_2O$ (6.5 mL) before the addition of $KHF_2$ (1.62 g; 20.7 mmol; 4 equiv.). The resulting mixture was stirred at ambient temperature for 3.5 hours before being concentrated under reduced pressure at 40 °C to give 4.4 g of a pale yellow solid. The resulting residue was crystallized from acetone and $Et_2O$. The obtained white solids (168 mg) were used without further purification and characterization.

**Synthesis of 6-(2-(9H-carbazol-9-yl)ethyl)-2,2-dimethyl-2H-chromene-8-carbaldehyde:**

6-bromo-2,2-dimethyl-2H-chromene-8-carbaldehyde (57 mg; 0.21 mmol; 1.0 equiv.), 9-(2-(trifluoro-λ$^4$-boraneyl)ethyl)-9H-carbazole potassium salt (64 mg; 0.21 mmol; 1.0 equiv.), $PdCl_2$(dppf).DCM (8 mg; 0.011 mmol; 0.05 equiv.) and $Cs_2CO_3$ were taken up in 1,5 mL toluene. An amount of 0.5 mL $H_2O$ was added and the mixture was stirred overnight at 80 °C. The mixture was allowed to cool to ambient temperature and subsequently poured into brine (20 mL) and extracted with EtOAc (25 mL).

The organic layer was collected, dried ($Na_2SO_4$), filtered and concentrated to dryness *in vacuo* at 40 °C to give 74 mg of an orange oil. The obtained crude was adsorbed onto Celite and subjected to silica gel flash chromatography eluting with 0% to 50% EtOAc in heptane to yield 29 mg of the desired product as a colourless oil.

$^1$H-NMR (300 MHz, $CDCl_3$) δ: 10.44 (s, 1H), 8.13 – 8.07 (m, 2H), 7.56 (d, *J* = 2.3 Hz, 1H), 7.43 (ddd, *J* = 8.3, 7.1, 1.2 Hz, 2H), 7.31 (d, *J* = 8.2 Hz, 2H), 7.23 (ddd, *J* = 8.0, 7.2, 1.0 Hz, 2H), 6.73 (d, *J* = 2.3 Hz, 1H), 6.14 (d, *J* = 9.9 Hz, 1H), 5.65 (d, *J* = 9.9 Hz, 1H), 4.49 (t, *J* = 7.4 Hz, 2H), 3.04 (t, *J* = 7.7 Hz, 2H), 1.47 (s, 6H) (Figure 1D and Supplementary Figure 2C). $^{13}$C-NMR (75 MHz, $CDCl_3$) δ: 189.2, 155.1, 140.0, 132.7, 131.6, 130.8, 126.5, 125.6, 124.1, 122.9, 122.5, 121.2, 120.3, 118.9, 108.5, 77.6, 44.6, 34.1, 28.0. HRMS [ESI+.]: found 382.1817, calculated 382.1807 for $C_{26}H_{23}NO_2$ $[M+H]^+$ (data not shown).

**Figure Legends**

Figure 1. Differences in response upon pan-PKC inhibition and B106 incubation in GNAQ/11 mutated and wild type cells. (A) Cell viability assay in which uveal melanoma cell lines MEL202 and MEL290 and cutaneous melanoma cell line FM6 were incubated with pan-PKC inhibitory drugs Sotrastaurin, GFX or selective PKCδ inhibitor B106 for 3 days. (B) Effects of 1 μM Sotrastaurin and 1 μM B106 after 24-hour incubation on the cell cycle profile of MEL202, MEL290 and FM6. (C) Western blot analysis of effects induced by 4 μM B106 (B) and 1 μM Sotrastaurin (S) compared to solvent DMSO (D) after 2-hour incubation on the amount of phosphorylated-PKCδ, -PKCδθ, -MARCKS and -JNK. Vinculin expression was analysed to ensure equal loading. (D) $^1$H-NMR confirmed structure of synthesized B106.

**Acknowledgements**

The authors like to thank G van der Heden for carefully reviewing the manuscript and thoughtful discussions.

**Supporting Information**

The Supporting Information is available free of charge at http://pubs.acs.org

- data supporting the results of Figure 1 by extending to other cell lines
- 1H-NMR conformation of B106 synthesis
- full results of Kinome Profiling of B106

## References


1. Van Raamsdonk, C. D., Griewank, K. G., Crosby, M. B., Garrido, M. C., Vemula, S., Wiesner, T., Obenauf, A. C., Wackernagel, W., Green, G., Bouvier, N., Sozen, M. M., Baimukanova, G., Roy, R., Heguy, A., Dolgalev, I., Khanin, R., Busam, K., Speicher, M. R., O'Brien, J., and Bastian, B. C. (2010) Mutations in GNA11 in uveal melanoma, *N Engl J Med 363*, 2191-2199.
2. Van Raamsdonk, C. D., Bezrookove, V., Green, G., Bauer, J., Gaugler, L., O'Brien, J. M., Simpson, E. M., Barsh, G. S., and Bastian, B. C. (2009) Frequent somatic mutations of GNAQ in uveal melanoma and blue naevi, *Nature 457*, 599-602.
3. Chen, X., Wu, Q., Depeille, P., Chen, P., Thornton, S., Kalirai, H., Coupland, S. E., Roose, J. P., and Bastian, B. C. (2017) RasGRP3 Mediates MAPK Pathway Activation in GNAQ Mutant Uveal Melanoma, *Cancer Cell 31*, 685-696 e686.
4. Feng, X., Degese, M. S., Iglesias-Bartolome, R., Vaque, J. P., Molinolo, A. A., Rodrigues, M., Zaidi, M. R., Ksander, B. R., Merlino, G., Sodhi, A., Chen, Q., and Gutkind, J. S. (2014) Hippo-independent activation of YAP by the GNAQ uveal melanoma oncogene through a trio-regulated rho GTPase signaling circuitry, *Cancer Cell 25*, 831-845.
5. Yu, F. X., Luo, J., Mo, J. S., Liu, G., Kim, Y. C., Meng, Z., Zhao, L., Peyman, G., Ouyang, H., Jiang, W., Zhao, J., Chen, X., Zhang, L., Wang, C. Y., Bastian, B. C., Zhang, K., and Guan, K. L. (2014) Mutant Gq/11 promote uveal melanoma tumorigenesis by activating YAP, *Cancer Cell 25*, 822-830.
6. Amirouchene-Angelozzi, N., Nemati, F., Gentien, D., Nicolas, A., Dumont, A., Carita, G., Camonis, J., Desjardins, L., Cassoux, N., Piperno-Neumann, S., Mariani, P., Sastre, X., Decaudin, D., and Roman-Roman, S. (2014) Establishment of novel cell lines recapitulating the genetic landscape of uveal melanoma and preclinical validation of mTOR as a therapeutic target, *Mol Oncol 8*, 1508-1520.
7. Wu, X., Li, J., Zhu, M., Fletcher, J. A., and Hodi, F. S. (2012) Protein kinase C inhibitor AEB071 targets ocular melanoma harboring GNAQ mutations via effects on the PKC/Erk1/2 and PKC/NF-kappaB pathways, *Mol Cancer Ther 11*, 1905-1914.
8. Wu, X., Zhu, M., Fletcher, J. A., Giobbie-Hurder, A., and Hodi, F. S. (2012) The protein kinase C inhibitor enzastaurin exhibits antitumor activity against uveal melanoma, *PLoS One 7*, e29622.
9. Piperno-Neumann, S., Kapiteijn, E., Larkin, J., Carvajal, R. D., Luke, J. J., Seifert, H., Roozen, I., Zoubir, M., Yang, L., Choudhury, S., Yerramilli-Rao, P., Hodi, F. S., and Schwartz, G. K. (2014) Phase I dose-escalation study of the protein kinase C (PKC) inhibitor AEB071 in patients with metastatic uveal melanoma, In *ASCO annual meeting 2014*, J. Clin. Oncol (abstr 9030).
10. Heijkants, R. C., Nieveen, M., Hart, K. C., Teunisse, A., and Jochemsen, A. G. (2018) Targeting MDMX and PKCdelta to improve current uveal melanoma therapeutic strategies, *Oncogenesis 7*, 33.
11. Takashima, A., English, B., Chen, Z., Cao, J., Cui, R., Williams, R. M., and Faller, D. V. (2014) Protein kinase Cdelta is a therapeutic target in malignant melanoma with NRAS mutation, *ACS Chem Biol 9*, 1003-1014.
12. Jager, M. J., Magner, J. A., Ksander, B. R., and Dubovy, S. R. (2016) Uveal Melanoma Cell Lines: Where do they come from? (An American Ophthalmological Society Thesis), *Trans Am Ophthalmol Soc 114*, T5.
13. Chen, X., Wu, Q., Tan, L., Porter, D., Jager, M. J., Emery, C., and Bastian, B. C. (2014) Combined PKC and MEK inhibition in uveal melanoma with GNAQ and GNA11 mutations, *Oncogene 33*, 4724-4734.
14. Evenou, J. P., Wagner, J., Zenke, G., Brinkmann, V., Wagner, K., Kovarik, J., Welzenbach, K. A., Weitz-Schmidt, G., Guntermann, C., Towbin, H., Cottens, S., Kaminski, S., Letschka, T., Lutz-Nicoladoni, C., Gruber, T., Hermann-Kleiter, N., Thuille, N., and Baier, G. (2009) The Potent Protein Kinase C-Selective Inhibitor AEB071 (Sotrastaurin) Represents a New Class of Immunosuppressive Agents Affecting Early T-Cell Activation, *Journal of Pharmacology and Experimental Therapeutics 330*, 792-801.
15. Soltoff, S. P. (2007) Rottlerin: an inappropriate and ineffective inhibitor of PKC delta, *Trends Pharmacol Sci 28*, 453-458.

16. Davies, S. P., Reddy, H., Caivano, M., and Cohen, P. (2000) Specificity and mechanism of action of some commonly used protein kinase inhibitors, *Biochem J 351*, 95-105.
17. Soltoff, S. P. (2001) Rottlerin is a mitochondrial uncoupler that decreases cellular ATP levels and indirectly blocks protein kinase Cdelta tyrosine phosphorylation, *J Biol Chem 276*, 37986-37992.
18. Liang, T., Zhang, X., Xue, W., Zhao, S., Zhang, X., and Pei, J. (2014) Curcumin induced human gastric cancer BGC-823 cells apoptosis by ROS-mediated ASK1-MKK4-JNK stress signaling pathway, *Int J Mol Sci 15*, 15754-15765.
19. van den Berg, M. C., van Gogh, I. J., Smits, A. M., van Triest, M., Dansen, T. B., Visscher, M., Polderman, P. E., Vliem, M. J., Rehmann, H., and Burgering, B. M. (2013) The small GTPase RALA controls c-Jun N-terminal kinase-mediated FOXO activation by regulation of a JIP1 scaffold complex, *J Biol Chem 288*, 21729-21741.
20. Abdel-Halim, M., Diesel, B., Kiemer, A. K., Abadi, A. H., Hartmann, R. W., and Engel, M. (2014) Discovery and optimization of 1,3,5-trisubstituted pyrazolines as potent and highly selective allosteric inhibitors of protein kinase C-zeta, *J Med Chem 57*, 6513-6530.
21. Kwiatkowski, J., Liu, B., Tee, D. H. Y., Chen, G., Ahmad, N. H. B., Wong, Y. X., Poh, Z. Y., Ang, S. H., Tan, E. S. W., Ong, E. H., Nurul, D., Poulsen, A., Pendharkar, V., Sangthongpitag, K., Lee, M. A., Sepramaniam, S., Ho, S. Y., Cherian, J., Hill, J., Keller, T. H., and Hung, A. W. (2018) Fragment-Based Drug Discovery of Potent Protein Kinase C Iota Inhibitors, *J Med Chem 61*, 4386-4396.
22. Chen, P. W., Murray, T. G., Uno, T., Salgaller, M. L., Reddy, R., and Ksander, B. R. (1997) Expression of MAGE genes in ocular melanoma during progression from primary to metastatic disease, *Clin Exp Metastasis 15*, 509-518.